Depletion-Induced Percolation in Networks of Nanorods

T. Schilling,[1] S. Jungblut,[1] and Mark A. Miller[2]

[1]*Institut für Physik, Johannes Gutenberg-Universität, D-55099 Mainz, Staudinger Weg 7, Germany*
[2]*University Chemical Laboratory, Lensfield Road, Cambridge CB2 1EW, United Kingdom*

(Received 11 May 2006; published 9 March 2007)

Above a certain density threshold, suspensions of rodlike colloidal particles form system-spanning networks. Using Monte Carlo simulations, we investigate how the depletion forces caused by spherical particles affect these networks in isotropic suspensions of rods. Although the depletion forces are strongly anisotropic and favor alignment of the rods, the percolation threshold of the rods decreases significantly. The relative size of the effect increases with the aspect ratio of the rods. The structural changes induced in the suspension by the depletant are characterized in detail and the system is compared to an ideal fluid of freely interpenetrable rods.

DOI: 10.1103/PhysRevLett.98.108303 PACS numbers: 82.70.Dd, 61.20.Ja, 64.60.Ak

Networks of electrically conducting carbon nanotubes (CNTs) have important applications in the development of lightweight conducting composites and films [1–5]. At equilibrium, colloidal suspensions of CNTs contain clusters with a distribution of sizes. Contiguous conducting paths first appear on a macroscopic scale when the CNT density crosses the percolation threshold, at which the average cluster size diverges. The sample's conductivity rises sharply by several orders of magnitude at this point [1–5]. The large aspect ratio of CNTs means that, for a disordered distribution of positions and orientations, a single particle provides connectivity over a longer distance than several more spherical particles with the same total volume. Hence, an insulating matrix can be loaded with a smaller volume fraction of conducting filler, leading to a lighter material.

The percolation threshold of the CNTs depends both on their aspect ratio, and on the interactions between them. Recent studies show that the addition of surfactant to a suspension of CNT bundles (CNTBs) substantially lowers the percolation threshold [6]. At sufficiently high concentrations, the surfactant self-assembles into micelles, which induce depletion attraction between the bundles [7]. Since the attraction is weak, percolation is reversible and the system remains at thermodynamic equilibrium, in contrast to strongly interacting particles, which may form structurally arrested gels [8].

The depletion forces arise from competition between the translational and orientational entropy of the CNTBs on the one hand, and the translational entropy of the micelles on the other. If two bundles approach closely, the volume available to micelles increases, inducing an effective attraction between bundles. The effect is highly anisotropic, since the volume excluded to the depletant depends on the relative orientations of the bundles [9,10]. The excluded volume is minimized in parallel arrangements of neighboring rods, but alignment also reduces the spatial extent of a cluster, and should therefore suppress rather than enhance the formation of percolating networks [11]. Even in systems of spheres, it is possible for attraction to raise the percolation threshold [12]. Nevertheless, recent analytic work on mixtures of rods and spherical depletants predicts that depletion does lower the percolation threshold of the rods for all depletant concentrations [13]. Depletion has also been implicated in enhanced percolation in binary mixtures of adhesive spheres [14]. Unlike purely theoretical treatments [13], our simulation approach takes full account of the angular correlations between neighboring rods—a crucial property of these highly anisotropic particles. We will see that depletion induces relatively local changes in the structure of an isotropic suspension of rods, but that these changes significantly affect the extent of clustering and therefore the position of the percolation threshold.

We model the CNTBs as hard spherocylinders, i.e., cylinders of length L and diameter D capped by hemispheres. To make as few assumptions as possible about the effect of depletion, we model the surfactant micelles explicitly rather than by employing an effective potential. Explicit representation has the advantage of automatically including many-body effects, due to multiple exclusion of the same volume, which can never be perfectly accounted for by a pair potential. In the experiments, the effective diameters of CNTBs and micelles are comparable [6,7], and we therefore model the micelles as hard spheres of diameter D. The range of the depletion interaction does depend on the depletant size, but for a given sphere volume fraction, a spot check at aspect ratio $L/D = 10$ revealed only a 2% change in the percolation threshold using sphere diameters of $0.5D$ to $1.3D$.

Similar mixtures have been the subject of other theoretical and simulation studies [9,10,15]. In particular, the phase diagram for low volume fractions and roughly equal rod and sphere diameters was studied within the second virial approximation by Matsuyama and Kato [16]. Most other studies, however, have been concerned with different regimes, either where the rods are in a liquid crystalline, rather than isotropic phase [17], or where the rods are

regarded as the depletant rather than the spheres [18–20]. We believe the present work to be the first time that depletion-induced percolation has been simulated in rod-sphere mixtures.

Monte Carlo simulations were performed at fixed volume and number of particles using single-particle displacements and rotations. The hard potential reduces the Monte Carlo acceptance criterion to the rejection of any trial move that generates an overlap between rods and/or spheres. A special cell system [21] was employed for efficient overlap detection. A cubic simulation box of volume $V = (5L)^3$ (except where stated) with periodic boundary conditions was used. A typical simulation involved 5×10^5 trial moves per particle (sweeps) for equilibration and a further 5×10^5 for sampling. Overall alignment of the rods was monitored using the nematic order parameter S, i.e., the largest eigenvalue of the tensor $\mathbf{Q} = (2N_r)^{-1} \sum_i^{N_r} (3\hat{\mathbf{u}}_i\hat{\mathbf{u}}_i - \mathbf{I})$. Here, $\hat{\mathbf{u}}_i$ is a unit vector along the axis of rod i, $\mathbf{I}$ is the identity matrix, and the sum is over all N_r rods. S is unity in a fully aligned configuration and zero in a perfectly isotropic fluid.

To define clusters of rods, a connectivity criterion is required. We are not concerned with details of electrical conductivity at CNTB contacts, and regard two rods to be connected if their surfaces approach closer than $0.2D$, or equivalently, if the line segments at the spherocylinders' axes approach closer than $A = 1.2D$. Although increasing A decreases the volume fraction for percolation, the percentage change due to the addition of spheres is not very sensitive to A. A cluster was counted as percolating if its particles were connected to their own periodic images. Percolation was tested every 20 sweeps.

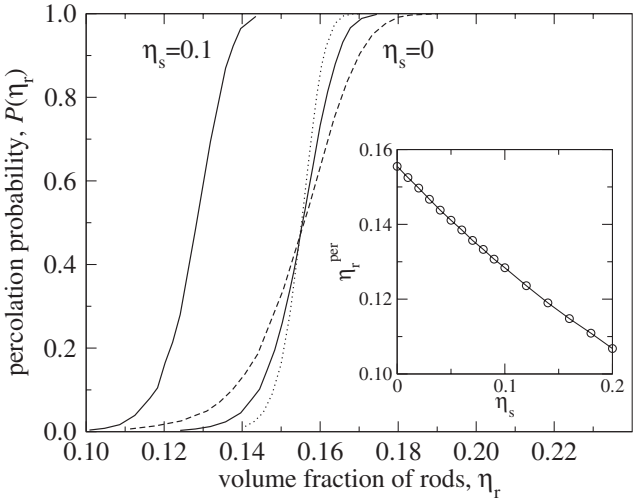

FIG. 1. Solid lines: percolation probability as a function of rod volume fraction for $L/D = 6$ and two sphere volume fractions η_s in a box of edge $5L = 30D$. Dashed and dotted lines: equivalent results for $\eta_s = 0$ only at box lengths $20D$ and $45D$, respectively. A typical uncertainty in $P(\eta_r)$ is 0.004. Inset: percolation threshold as a function of η_s for $L/D = 6$.

The aspect ratio of CNTBs can exceed 100, which is beyond the reach of our simulations. However, the emergence of long-rod behavior in the rod-sphere mixture becomes clear by simulating increasing L/D starting from relatively small values. Figure 1 demonstrates the effect of depletion forces on the percolation of rods with $L/D = 6$. The equilibrium probability $P(\eta_r)$ of finding a percolating cluster is plotted as a function of the rod volume fraction $\eta_r = N_r v_h/V$, where N_r is the number of rods and $v_h = \pi D^3(2 + 3L/D)/12$ is the volume of a rod's hard core. Addition of a volume fraction $\eta_s = 0.1$ of spheres shifts $P(\eta_r)$ to lower rod volume fraction by 17.5%.

In an infinite system, $P(\eta_r)$ would rise instantaneously at the percolation threshold, but the simulations measure a sigmoidal curve whose width decreases with increasing box size due to finite size effects, as demonstrated for the pure rod case in Fig. 1. Nevertheless, the volume fraction at which $P(\eta_r)$ passes through 0.5 is almost independent of the cell size and we therefore adopt $P(\eta_r^{per}) = 0.5$ as a robust definition of the percolation threshold η_r^{per}. Above the sharp onset of percolation at η_r^{per}, the conductivity rises as $(\eta_r - \eta_r^{per})^t$ [22], where the critical exponent t may depend on the rod aspect ratio [23].

As expected, η_r^{per} is lower for longer rods, as shown for a selection of L/D ratios in Table I. Data are given for rods with no depletant, and with a volume fraction $\eta_s = 0.03$ of spheres, which is comparable to the highest concentration of micelles used in Ref. [6]. The fractional decrease δ in the percolation threshold due to the spheres is 5.2% at $L/D = 4$, rising gradually to 8.3% by $L/D = 25$ in contrast to theoretical predictions of constant δ [13]. The increasing shift is likely to continue as the aspect ratio rises towards that typical of CNTBs. However, if a scaling regime of the form $\eta_r^{per} \propto (L/D)^{-a}$ is entered for sufficiently long rods, and the value of a is not affected by the presence of spheres, then the fractional drop in η_r^{per} caused by a given volume fraction of spheres would eventually become independent of the aspect ratio.

TABLE I. Percolation threshold for selected aspect ratios L/D at two sphere volume fractions η_s. η_r^{per} is the volume fraction of rods at percolation, and n^{per} is the average number of (rod) neighbors per rod, averaged over all rods in the system. δ is the fractional decrease in η_r^{per} caused by sphere volume fraction $\eta_s = 0.03$.

	$\eta_s = 0$		$\eta_s = 0.03$		
L/D	η_r^{per}	n^{per}	η_r^{per}	n^{per}	δ
4	0.1784	1.61	0.1691	1.63	0.052
6	0.1555	1.54	0.1467	1.56	0.057
10	0.1236	1.45	0.1156	1.47	0.065
17	0.0911	1.35	0.0844	1.37	0.074
25	0.0702	1.29	0.0644	1.30	0.083

In fact, such a scaling has been predicted for ideal systems of freely interpenetrable rods. In the hope of estimating percolation thresholds without the need for detailed calculation, several quantities have been suggested as approximate dimensional invariants at the threshold. Candidates included the number of bonds per particle, the total excluded volume [24,25], and the zero of the Euler characteristic [26]. Although none of these approaches works universally well for arbitrary particle shapes and mixtures, the quantity $\rho^{\mathrm{per}}\langle v_{\mathrm{ex}}\rangle$ is an approximate invariant for ideal rods [23], where ρ^{per} is the number density at percolation and $\langle v_{\mathrm{ex}}\rangle$ is the so-called excluded volume (orientationally averaged) that would be inaccessible to the center of one particle due to the presence of another if overlaps were forbidden. Defining the total critical volume by $V_c = \rho^{\mathrm{per}} v$, where v is the volume of an ideal rod, the invariant becomes $V_c\langle v_{\mathrm{ex}}\rangle/v$. For long rods, $\langle v_{\mathrm{ex}}\rangle/v \propto L$ and hence $V_c \propto 1/L$.

Ideal rods rapidly enter this scaling regime [23], as shown by the dotted line in Fig. 2. Each evaluation of the percolation probability was obtained from 10 000 uncorrelated and randomly generated configurations of line segments, using the same box size and connectivity criterion as in the spherocylinder simulations. The introduction of a hard core induces local structure into the isotropic fluid and rules out a large fraction of percolating ideal configurations, raising the percolation threshold (solid line, Fig. 2). For the aspect ratios accessible to our simulations, no power-law scaling is observed. However, the theoretical reference interaction site model (RISM) predicts that the effect of a hard core is to postpone scaling to larger aspect ratios and that $1/L$ scaling is eventually recovered [27]. The RISM results (long-dashed line, Fig. 2) and the simulations without spheres (solid line) approach each other for large L/D.

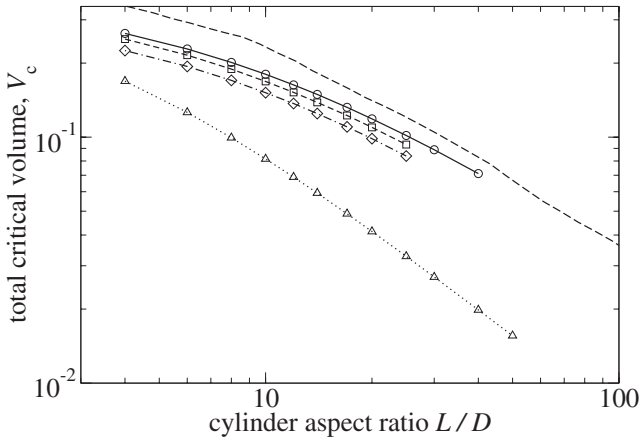

FIG. 2. Dependence of the total critical volume on the aspect ratio of the rods for sphere volume fractions $\eta_s = 0$ (solid line) and $\eta_s = 0.03$ (short-dashed line for clusters of rods only and dot-dashed line when spheres are included), and for the ideal system of freely interpenetrable rods (dotted line). The long-dashed line shows RISM results for $\eta_s = 0$ from Ref. [27].

Table I shows a decline in the rate of increase of δ with L/D, and in the scaling regime δ would level out to a constant. A linear extrapolation of δ to experimental aspect ratios starting at $L/D = 200$ [6] therefore provides a crude upper bound to the contribution of pure entropy in the CNTB-micelle experiments. The extrapolation predicts a lowering of 30–40%, a sizeable effect but far smaller than the experimental one. The additional influence of direct energetic interactions in the CNTB suspension could be tested by replacing the micelles by a different depletion agent with the same excluded volume. Conceivably, micelles could also contribute to conductivity. However, as shown by the dot-dashed line in Fig. 2, including spheres in the cluster definition shifts the percolation threshold by less than 10%.

We now turn to structural characteristics of the fluid. In all the simulations the rods remain in the isotropic phase, which has no long-range order in either the center-of-mass positions or the alignment of the rods. However, the hard interactions give rise to local structure, which is affected by the addition of hard spheres. Local alignment is revealed by the orientational correlation function $g_2(r) = \langle P_2(\hat{\mathbf{u}}_i \cdot \hat{\mathbf{u}}_j)\rangle_r$, where $P_2(x) = (3x^2 - 1)/2$ is the second Legendre polynomial, and the averaging is restricted to pairs of rods whose centers are separated by $r_{ij} = r$. As shown in Fig. 3(a), $g_2(r)$ decays to zero in an isotropic fluid, but becomes positive when rods approach closely enough to restrict each other's rotation.

The addition of hard spheres to the rods encourages nearby rods to align, since alignment decreases the total volume excluded to the spheres by an amount proportional to the length of the adjacent segment, thereby increasing the entropy of the spheres at the expense of some orientational entropy of the rods. Figure 3(a) shows that the spheres greatly enhance alignment of rods with nearby centers and (inset) that the centers are pushed closer together. The range of the effect is on the order of the sphere diameter D and decays to the underlying correlation, whose range depends on L. For sphere concentrations $\eta_s = 0.03$ around those of the micelles in Ref. [6], there is very little increase in alignment beyond the range D, and no significant bundling of spherocylinders was observed. At higher η_r, the spread of depletion-induced alignment lowers the bulk isotropic-nematic transition density [10], but following the percolation line $\eta_r^{\mathrm{per}}(\eta_s)$ (inset of Fig. 1), we find that the nematic is preempted by rod-sphere demixing (around $\eta_s = 0.22$ for $L/D = 6$).

Crucial to cluster formation and percolation is the probability distribution $p(d)$ of shortest distances d between pairs of rod axes, since it is the criterion $d < A$ that defines contact. To reveal the effect of the hard potential on the structure, we divide $p(d)$ by the equivalent distribution $p_{\mathrm{id}}(d)$ for ideal rods. The ratio $p(d)/p_{\mathrm{id}}(d)$ is plotted in

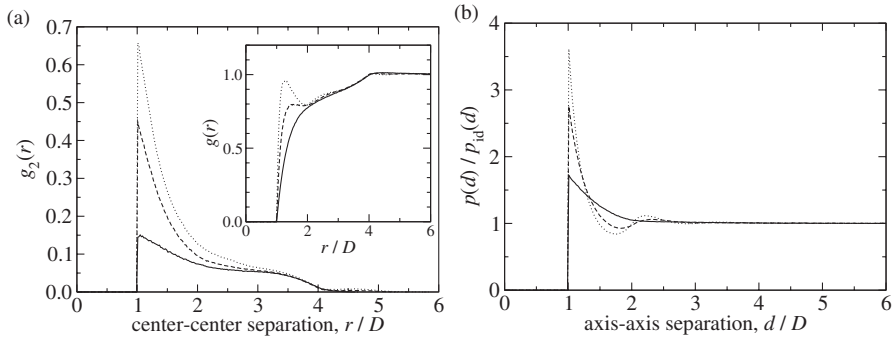

FIG. 3. Fluid local structure for $L/D = 6$ at volume fraction $\eta_r = 0.142$. (a) Orientational correlation function $g_2(r)$, inset: radial distribution function, $g(r)$, (b) distribution $p(d)$ of axis-axis separations normalized by the ideal distribution $p_{id}(d)$. Results for three sphere volume fractions are shown: $\eta_s = 0$ (solid lines), $\eta_s = 0.1$ (dashed lines) and $\eta_s = 0.15$ (dotted lines).

Fig. 3(b). As with the first peak in the radial distribution function of a simple fluid, the distribution of axis-axis separations rises above the random distribution for small d. The addition of hard spheres again has a large but short-ranged effect on the distribution, pushing the rods together at any point of approach along their lengths. For the high sphere volume fraction of $\eta_s = 0.15$ a small second peak emerges at $d \approx 2.2D$, indicating a weak correlation between two contacts with an intervening rod or sphere. The enhancement of $p(d)$ by the spheres for separations $d < A$ is a highly localized adjustment to the structure of the pure rod fluid, but increases the connectivity enough to cause the cluster size to diverge at lower rod concentration.

The average number n^{per} of contacts per rod at percolation (Table I), decreases with the aspect ratio, confirming that, as for ideal objects, this quantity is not an invariant [23,25,26]. The number of contacts is a sensitive function of the rod density, so it is interesting to note that n^{per} has similar values at $\eta_s = 0$ and 0.03; the spheres lower the percolation threshold, but they increase the number of contacts per rod at the lowered threshold roughly to its percolation value in their absence. The low n^{per} for long rods show how sparsely connected the network is at the onset of percolation, but the strength of the network continues to increase sharply above η_r^{per}.

Using a simple model of hard spherocylinders and spheres, we have isolated the effect of depletion on the percolation threshold of nanorod networks. The spheres induce pronounced but short-ranged changes in the structure of the isotropic rod fluid, including enhanced local alignment. At depletant concentrations relevant to experimental work on suspensions of carbon nanotubes and micelles [6], the alignment is too weak to cause global nematic order or significant aggregation of rods. Although pairs of particles extend less far when mutually aligned, depletion enhances contacts at all positions along the rods, leading to larger clusters and a decrease in the percolation threshold. It should therefore be possible to enhance the percolation of nanorods using depletants other than micelles, such as polymer coils or latex spheres. The fractional decrease caused by a given volume fraction of depletant gradually increases with the aspect ratio of the rods. This prediction could, in principle, be tested if shorter nanorods can be synthesized and characterized.

We are grateful to the DFG (No. Tr6/D5 and Emmy Noether Program), the MWFZ and EPSRC for support. We thank K. Binder, P. Poulin, T. Gruhn, M. Oettel, and E. Frey for helpful discussions.

[1] J. Coleman *et al.*, Phys. Rev. B **58**, R7492 (1998).
[2] J. Sandler *et al.*, Polymer **40**, 5967 (1999).
[3] J. M. Benoit, B. Corraze, and O. Chauvet, Phys. Rev. B **65**, 241405(R) (2002).
[4] P. Pötschke, S. Dudkin, and I. Alig, Polymer **44**, 5023 (2003).
[5] B. Vigolo *et al.*, Science **290**, 1331 (2000).
[6] B. Vigolo *et al.*, Science **309**, 920 (2005).
[7] H. Wang *et al.*, Nano Lett. **4**, 1789 (2004).
[8] A. Mohraz, D. B. Moler, R. M. Ziff, and M. J. Solomon, Phys. Rev. Lett. **92**, 155503 (2004).
[9] W. Li and H. R. Ma, Eur. Phys. J. E **16**, 225 (2005).
[10] S. V. Savenko and M. Dijkstra, Phys. Rev. E **70**, 051401 (2004).
[11] S. H. Munson-McGee, Phys. Rev. B **43**, 3331 (1991).
[12] A. L. R. Bug, S. A. Safran, G. S. Grest, and I. Webman, Phys. Rev. Lett. **55**, 1896 (1985).
[13] X. Wang and A. Chatterjee, J. Chem. Phys. **118**, 10787 (2003).
[14] Y. C. Chiew and E. D. Glandt, J. Phys. A **22**, 3969 (1989).
[15] R. Roth *et al.*, Phys. Rev. Lett. **89**, 088301 (2002).
[16] A. Matsuyama and T. Kato, Eur. Phys. J. E **6**, 15 (2001).
[17] P. van der Schoot, J. Chem. Phys. **117**, 3537 (2002).
[18] Y. Chen and K. Schweizer, J. Chem. Phys. **117**, 1351 (2002).
[19] S. Oversteegen, J. Wijnhoven, C. Vonk, and H. N. W. Lekkerkerker, J. Phys. Chem. B **108**, 18158 (2004).
[20] P. Bolhuis, J. Brader, and M. Schmidt, J. Phys. Condens. Matter **15**, S3421 (2003).
[21] R. L. C. Vink and T. Schilling, Phys. Rev. E **71**, 051716 (2005).
[22] D. Stauffer and A. Aharony, *Introduction to Percolation Theory* (Taylor & Francis, London, 1994), 2nd ed.
[23] M. Foygel *et al.*, Phys. Rev. B **71**, 104201 (2005).
[24] I. Balberg, C. H. Anderson, S. Alexander, and N. Wagner, Phys. Rev. B **30**, 3933 (1984).
[25] G. E. Pike and C. H. Seager, Phys. Rev. B **10**, 1421 (1974).
[26] K. R. Mecke and A. Seyfried, Europhys. Lett. **58**, 28 (2002).
[27] K. Leung and D. Chandler, J. Stat. Phys. **63**, 837 (1991).